Sādhanā (2022)47:199
https://doi.org/10.1007/s12046-022-01971-7

The effects of flux particle size and column height on the bead geometry in submerged arc welding

JATINDER GARG[1], SONU BALA GARG[2,*], BIKRAM JEET[1] and HARMEET SINGH[3]

[1]Baba Hira Singh Bhattal Institute of Engineering and Technology, Lehragaga, Punjab 148031, India
[2]IK Gujral Punjab Technical University, Jalandhar, Punjab 144603, India
[3]Chandigarh University, Gharuan, Punjab, India
e-mail: sonugarg79@yahoo.com

MS received 26 July 2020; revised 13 August 2022; accepted 17 August 2022

Abstract. The weld bead geometry has a significant influence on the quality of welds in submerged arc welding (SAW). Much research has been undertaken to investigate the influence of various welding parameters like arc voltage, welding current, electrode diameter, wire stickout, travel speed, and welding polarity on the bead geometry in SAW welding process. But the effects of flux particle size and the flux column height are still largely uninvestigated. This paper presents a systematic investigation of the effects of flux particle size and column height on the bead geometry in the SAW process. The experiments were designed by central composite rotatable design (CCRD). Welding current, travel speed, flux particle size, and column height were taken as independent process variables. The experimental data was used to develop quadratic polynomial regression models for penetration, bead width, and reinforcement. After testing for their adequacy and fit, these models were used to understand the main and interactive effects of the process variables on the bead geometry. The results showed that both the flux particle size and column height significantly influence the bead geometry of the welds. A 100% increase in average particle size, reduced the bead width by 9% and increased the reinforcement by 12%. On the other hand, a 50% rise in the flux height elevated the bead width by 10% and reduced the reinforcement by 15%. However, the penetration remained unaffected by both these factors. Further, it was also found that a course flux coupled with a low flux column height could produce smoother weld beads with fine ripples, free from surface defects.

Keywords. Submerged arc welding; bead geometry; flux particle size; flux column height.

1. Introduction

Submerged arc welding is an arc welding process which is known for its very high productivity rate. This process uses loose granulated flux which surrounds the weld pool and the arc remains completely non-visible [1]. The arc, the electrode tip, and the welding zone remain surrounded and protected by the molten flux while the top layer of un-fused flux secures them all [2]. The most significant advantage of this process is its ability to draw a substantial amount of current, as a result of which it can achieve a very high metal deposition rate. Consequently, this process can weld even thick plates in a single pass [3, 4]. The other advantages like excellent surface appearance, deeper penetration, decent weld quality, absence of arc flashes and spatters, ease of automation, and lower welder skill requirement make this process a very popular choice in the manufacturing sector [5–7]. This process is also used for cladding and hard-facing [8]. Ever since the invention of the SAW process, efforts have been made to improve its productivity [9]. As a result, various high productivity methods like multiple wire welding [10], metal powder addition [11], hot and cold wire addition [12, 13], and the use of tubular flux/metal-cored electrodes [1, 14], have evolved.

The weld bead geometry has a significant influence on the quality of welds in submerged arc welding [15, 16]. The major elements of the bead geometry have been illustrated in figure 1. All these elements considerably affect the mechanical strength of the welds [17, 18]. The weld bead must have adequate penetration to provide sufficient bonding with the base metal. Improper bead geometry often leads to defects like lack of fusion and incomplete penetration, especially in multi-pass welds [7]. A very narrow bead with too much penetration may promote hot cracking [19]. Larger reinforcement coupled with higher welding speeds may induce centerline cracks in the welds. In applications where low dilution is needed, a weld bead with lesser penetration and greater reinforcement is often desired [20, 21]. All these factors call for maintaining an optimal balance between various elements of the bead geometry. It

*For correspondence
Published online: 05 October 2022

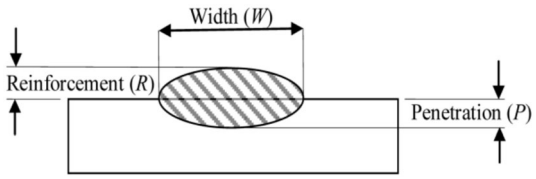

Figure 1. Major elements of weld bead geometry.

is also important to develop mathematical models that describe the influence of process variables on the bead geometry elements. This mathematical modelling assumes further importance for mechanized processes like submerged arc welding, where the process parameters are pre-selected to achieve the desired bead profile [15].

Several attempts have been made by scientists and researchers to develop mathematical models for bead geometry elements in terms of different process variables. Yang *et al* [22] conducted detailed experimentation to identify the process variables that affect the bead geometry. They found that the current, travel speed, arc voltage, electrode extension, weld polarity, and electrode diameter are the primary elements that influence the deposition rate. Chandel *et al* [7] theoretically illustrated the influence of change in melting rate on the bead profile in the SAW welding process. They further tried to elaborate on the detailed effects of various process parameters such as current, wire diameter, welding polarity and wire stickout on the bead profile. Tarng and Yang [23] developed a Taguchi-based methodology for finding the optimal values of the process variables for making a sound weld. He supported his study with experimental results. Gunaraj and Murugan [24, 25] developed mathematical models for the bead geometry of the welds made on large-diameter pipes. Sarkar *et al* [16] developed artificial neural networks (ANN) based on mathematical models that could be used to estimate the bead geometry and HAZ of the submerged arc welds. Kanjilal [26] conducted experiments to understand the joint influence of flux and process variables on chemistry, mechanical properties, and bead geometry. The author found that besides the individual effects, the combined effects of the process variables also have a profound influence on the bead profile. Karaoglu and Secgin [27] showed that even slight variations in the process parameters may induce large effects on the bead geometry of the welds. Choudhary *et al* [28] quantified the relationship between process variables like arc voltage, wire feed rate, travel speed, wire stickout and workpiece thickness with the bead geometry of SAW welds.

Therefore, it is evident that the efforts of a majority of the previous researchers were mainly focused on studying the influence of process variables like welding current, travel speed, wire stickout, arc voltage, weld polarity, and electrode diameter on the weld bead geometry and other quality characteristics of the Submerged arc welds. However, many authors [29] and practising engineers [30, 31] strongly believe that the flux particle size also significantly affects the bead geometry and surface appearance of the SAW welds. Similarly, a few authors [32, 33] have also pointed out that the flux column height, i.e. the height of the flux column above the weld pool, also exerts a significant influence on the physical characteristics of the SAW welds. However, no evidence of conducting any systematic research to establish these aspects could be found anywhere in the literature.

The research work presented in this paper was undertaken to fill this major gap. In this work, a systematic investigation was undertaken to ascertain if the flux particle size and the column height exert any significant influences on the bead geometry and surface finish of the SAW welds. Response surface methodology (RSM) with central composite rotatable design (CCRD) was employed for conducting the study. Statistical mathematical models were developed to quantify the direct and interactive effects of the process variables on the bead geometry elements.

2. Methodology

The experiments were conducted on ESAB Tornado M-800, an IGBT inverter-based submerged arc welding machine. AISI 1025 steel plates of 180 × 65 × 15 mm size were used as workpieces. EH-14 electrodes wire of 3.15 mm diameter along with Automelt A-55 aluminate-rutile type acidic agglomerated flux with a basicity index of 0.61, were used. Besides flux particle size and column height, the welding current and travel speed were taken as additional factors. The values of other process variables namely the open-circuit voltage and the nozzle to plate distance was kept constant at 30 V and 30 mm, respectively. All the experiments were carried out at DCEP i.e. the reverse polarity.

The experiment was designed by Response surface methodology (RSM) with a full factorial central composite rotatable design (five levels), to study the effects of four independent variables namely welding current (I), average flux particle size (G), flux column height above the weld pool (H) and the weld travel speed (S) on various elements of bead geometry i.e. penetration (p), bead width (w) and reinforcement (r). Design-Expert Software (V.11) was employed.

A list of design factors (independent variables) along with their coded and actual values at various levels have been shown in table 1. Since a full factorial design with four factors was used for designing the experiments, the value of alpha (α) was taken as 2 [34]. The original flux (A-55) was segregated into five grades by sieving with a set of six standard sieves (ASTM No. 7, 8, 12, 16, 20, and 45), shown in figure 2. These different grades had the same composition but differed in their average particle

Table 1. The design factors and their coded/actual values at various levels.

Factor	Notation	Coded levels				
		$-\alpha$	-1	0	$+1$	$+\alpha$
Welding current (A)	I	300	400	500	600	700
Flux particle size (mm)	G	0.5	1	1.5	2	2.5
Flux column height (mm)	H	15	20	25	30	35
Travel speed (m/min)	S	0.1	0.15	0.2	0.25	0.3

Figure 2. Set of standard sieves used for grading the flux.

size (2.5 mm, 2 mm, 1.5 mm, 1 mm and 0.5 mm). Figure 3 shows a close-up of these different grades of fluxes used in the study. The design matrix has been presented in table 2 in coded form. It contains a total of 30 sets of experiments out of which the first sixteen are factorial points, the next eight are star points and the last six are centre points. The experimental runs were conducted in a random order to avoid systematic error to creep into the observations.

Bead on plate were deposited with one bead per experiment. After cooling to room temperature, transverse sections of 20 mm width were removed from the centre of each workpiece, as shown in figure 4. These specimens were ground and etched as per the standard metallurgical procedure to reveal their bead geometries. The bead geometry of the specimens was scanned by a high-resolution scanner. The various elements of the bead geometry were measured in *Adobe Acrobat Pro DC* software [5]. The results have been presented in table 2.

3. Results and discussion

This experimental data was entered into the Design-Expert software to develop mathematical models for various elements of the bead geometry. The software tried to fit different types of regression models (linear, 2FI, quadratic and cubic) to the input data but recommended the use of second-order polynomial (quadratic) models, for all responses. For the given sets of data, the quadratic models obtained the highest F-values and least p-values, which indicated their best fit to the experimental data.

The quadratic polynomial mathematical models were developed for bead width (w), penetration (p), and reinforcement (r) in terms of welding current (I), average flux particle size (G), flux column height (H) and travel speed (S). The adequacy and fit of the models were checked by

Figure 3. The five grades of flux used for the study.

Table 2. The design matrix and values of responses.

		Coded factors				Response values		
Std	Run	Current (I) A	Particle size (G) mm	Column height (H) mm	Travel speed (S) m/min	Penetration (p) mm	Bead width (w) mm	Reinforcement (r) mm
1	20	−1	−1	−1	−1	5.73	18.92	5.01
2	6	1	−1	−1	−1	9.32	18.85	7.23
3	25	−1	1	−1	−1	5.94	17.24	5.49
4	5	1	1	−1	−1	9.42	17.38	7.81
5	15	−1	−1	1	−1	6.12	20.41	4.79
6	7	1	−1	1	−1	9.51	20.03	6.32
7	12	−1	1	1	−1	5.82	18.65	4.99
8	18	1	1	1	−1	9.59	18.43	6.59
9	2	−1	−1	−1	1	4.77	15.34	3.29
10	11	1	−1	−1	1	8.43	17.67	4.43
11	14	−1	1	−1	1	4.44	13.46	3.52
12	13	1	1	−1	1	8.51	16.03	4.68
13	3	−1	−1	1	1	4.57	17.28	2.93
14	16	1	−1	1	1	8.48	19.57	3.37
15	29	−1	1	1	1	4.63	15.71	3.44
16	21	1	1	1	1	8.53	17.96	3.82
17	10	−2	0	0	0	4.05	15.94	3.57
18	9	2	0	0	0	11.3	18.81	6.54
19	1	0	−2	0	0	6.71	18.89	3.72
20	23	0	2	0	0	6.79	15.82	4.86
21	22	0	0	− 2	0	6.84	17.56	5.62
22	27	0	0	2	0	6.54	20.26	4.12
23	24	0	0	0	− 2	8.55	19.44	7.62
24	17	0	0	0	2	6.28	15.47	2.53
25	26	0	0	0	0	6.74	15.75	3.55
26	19	0	0	0	0	6.43	16.71	3.99
27	8	0	0	0	0	5.97	15.43	4.26
28	28	0	0	0	0	5.69	16.19	3.68
29	4	0	0	0	0	6.01	16.92	4.22
30	30	0	0	0	0	5.52	16.39	3.81

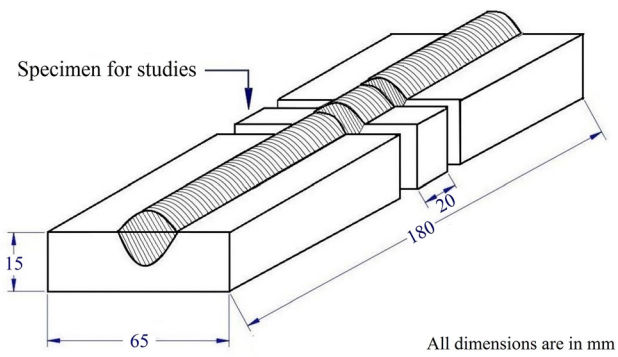

Figure 4. Schematic diagram for extraction of specimen from workpieces.

analysis of variance (ANOVA) techniques. The software calculated the regression coefficients of the linear, interactive and quadratic terms in the models. The significance of all the regression coefficients was tested by ANOVA by calculating their F and p-values. A p-value less than 0.05 signified that the corresponding model terms are significant and should be included in the final model. The insignificant coefficients were dropped from the final models along with their corresponding factors. The regression coefficients for various significant terms in all three mathematical models are shown in table 3. The finally obtained mathematical models for penetration (p), bead width (w), and reinforcement (r) have been presented in equations (1)-(3).

Table 3. Regression coefficients of significant terms in the mathematical models.

Regression coefficients	Penetration (p)	Bead width (w)	Reinforcement (r)
Intercept	6.38	16.23	3.92
Current (I)	1.84	0.6104	0.6971
Particle size (G)	–	− 0.8063	0.2187
Colum height (H)	–	0.7729	− 0.3421
Welding speed (S)	− 0.5679	− 1.03	− 1.21
IH	–	–	− 0.1806
IS	–	0.6231	− 0.2844
HS	–	0.1806	–
I^2	0.3601	0.2707	0.2899
G^2	–	0.2657	0.0986
H^2	–	0.6545	0.2436
S^2	0.2951	0.2907	0.2949
R^2	0.9728	0.9763	0.9886

$$\text{Penetration } (p) = 6.38 + 1.84I - 0.5679S + 0.3601I^2 + 0.2951S^2 \quad (1)$$

$$\text{Bead width } (w) = 16.23 + 0.6104I - 0.8063G + 0.7729H - 1.03S + 0.6231\ \text{IS} + 0.1806\ \text{HS} + 0.2707I^2 + 0.2657G^2 + 0.6545H^2 + 0.2907S^2 \quad (2)$$

$$\text{Reinforcement } (r) = 3.92 + 0.6971I + 0.2187G - 0.3421H - 1.21S - 0.1806IC - 0.2844IS + 0.2899I^2 + 0.0986G^2 + 0.2436H^2 + 0.2949S^2 \quad (3)$$

The scatter diagrams showing the predicted vs. actual values for bead width, penetration and reinforcement have been depicted in figure 5. From these figures, it can be observed that the predicted and observed values for all the response variables are in close agreement with each other, which further validates the developed models.

The direct and interactive effects of the process parameters on the bead geometry were estimated from the developed models. Their analysis and interpretations have been presented in the following subsections.

3.1 *Effects of welding current*

Based on Eq. 1 to 3, the graph shown in figure 6 was plotted between the welding current and the corresponding values of the bead geometry parameters. It shows that there is a positive correlation between the welding current and all three bead geometry parameters. As a result, an increase in the current improved the values of all these parameters.

In arc welding processes, an increase in welding current elevates the heat input to the weld pool and increases the melting rate [7, 22]. In submerged arc welding, the welding current (I) and the melting rate for a fixed-diameter electrode and a constant wire stickout are inter-related as per the following expression [7].

$$\text{Melting Rate } = AI + BI^2 + C \quad (4)$$

The values of constants A, B and C depend on the welding polarity, electrode material, electrode diameter, and electrode extension [22, 23]. In general, the first portion of this relation is related to the heat input of the electric arc, whereas the second part is concerned with the heat generated by resistive heating of the electrode [7]. An increase in the welding current is accompanied by an enhanced melting rate that manifests itself in the form of an increased reinforcement and weld width [25, 26]. At the same time, increased heat input to the weld pool triggers greater melting of the base material, that in turn improves the penetration [6].

In percentage terms, a 50% increase in the welding current (400 to 600 A) enhanced penetration by 60%, reinforcement by 40% and the bead width by 15%. The graph indicates an almost linear relationship between the welding current and the penetration of the weld bead. It is because, at a nominal electrode extension, the increased welding current causes an almost linear enhancement in the heat input, which increases the bead penetration and the metal deposition rate [7, 22, 23, 35].

Further, it can be observed that for the same increase in the current value, the improvement in bead width was

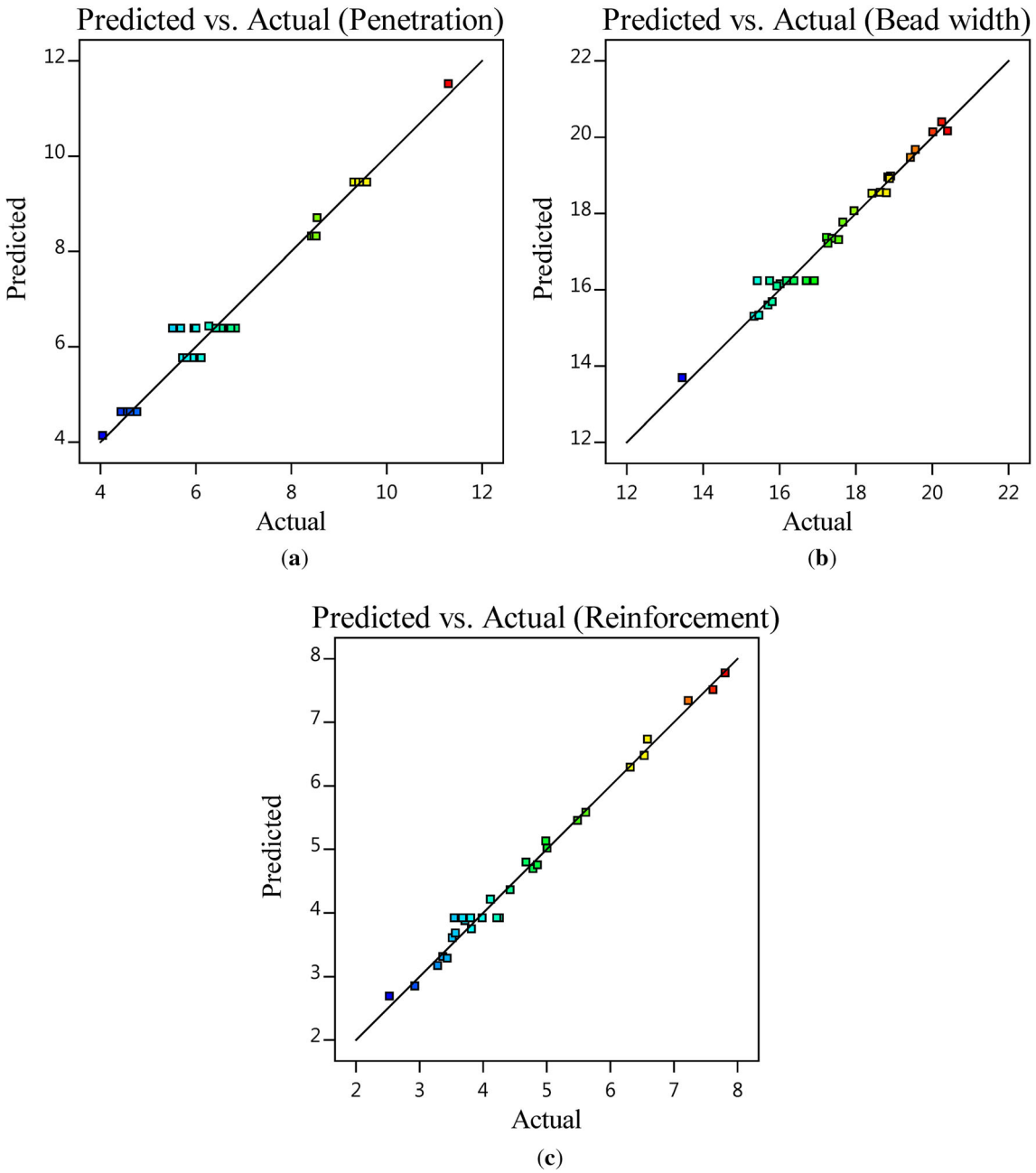

Figure 5. Scatter diagrams for (**a**) penetration, (**b**) bead width and (**c**) reinforcement.

relatively nominal. The bead width of the welds primarily depends on the arc voltage. An elevation in the arc voltage enhances the spread of the arc cone, which in turn increases the bead width [18, 24]. However, the increase in welding current does not change the arc voltage significantly. As a result, the bead width does not increase by a larger proportion. The 15% increase in the bead width is also primarily attributed to the increased heat input and the enhanced metal deposition rate [27, 36].

3.2 *Effects of flux particle size*

The effects of flux particle size on various bead geometry parameters have been summarized in the graph shown in figure 7.

Figure 7 shows that the flux particle size significantly influences the bead width and the reinforcement. However, it does not affect the penetration. From the graph, it can be noted that a 100% variation in the flux particle size (1 to 2 mm) decreased the bead width by 9% and increases the reinforcement by 12%.

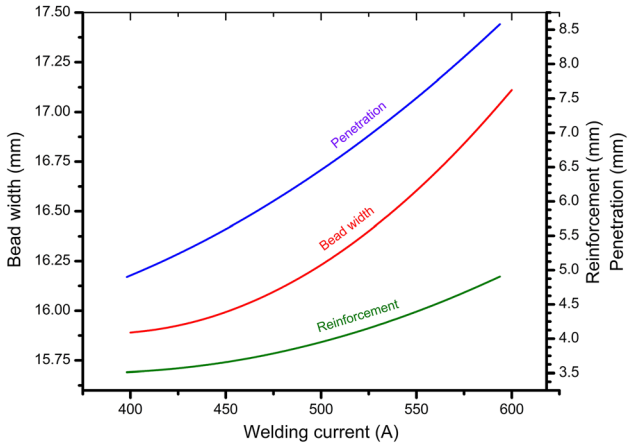

Figure 6. Influences of welding current.

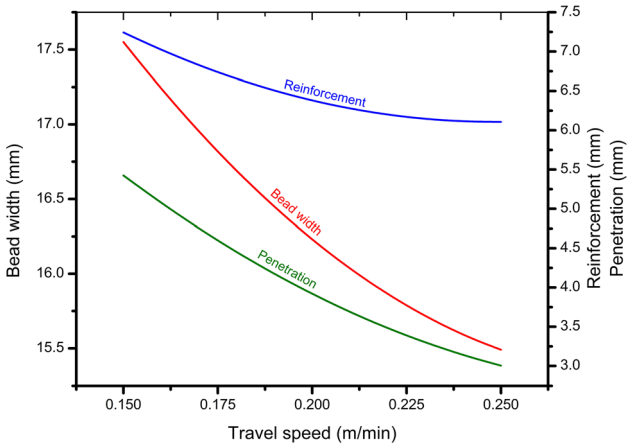

Figure 8. Influences of travel speed.

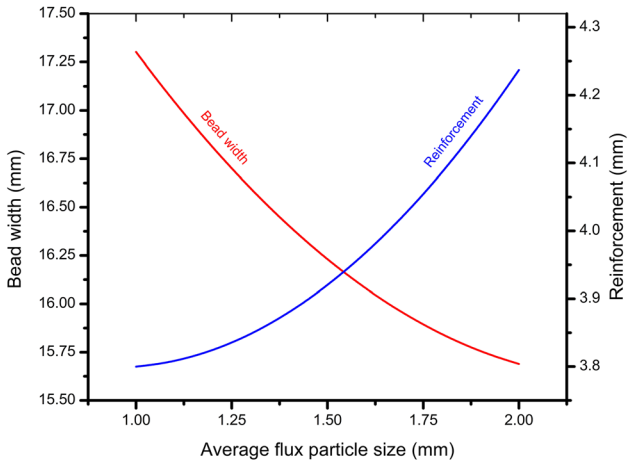

Figure 7. Influences of flux particle size.

As the size of flux particles decreases, they become finer and their interstitial space decreases. They become compactly packed and the density of the flux increases. As a result, the weight of the flux column above the molten weld pool increases. It exerts a larger downward force on the molten weld pool thereby reducing its reinforcement. Since the change in flux particle size does not affect the heat input of the welds, it does not change the penetration and the metal deposition rate [26]. As a result, the total volume of the molten metal remains the same. Since the penetration remains the same, the decrease in reinforcement causes a corresponding increase in the weld width. Therefore, the decrease in flux particle size enhances the bead width and reduces the reinforcement.

Apart from the above, the decrease in the average particle size reduces the permeability of the flux layer above the arc cavity. As a result, the gases produced in the arc cavity find it difficult to escape into the atmosphere. This increased gas pressure exerts a larger downward force on the molten weld pool, thereby causing a reduction in reinforcement and a corresponding enhancement in the bead width [32].

3.3 *Effects of travel speed*

In submerged arc welding, the weld travel speed significantly influences the bead geometry. Figure 8 shows the effect of travel speed on the bead geometry, as observed in this study.

From the graph, it can be observed that the travel speed exerts a negative influence on all the bead geometry parameters. A 67% increase in travel speed (0.15 to 0.25 m/min) reduced the penetration by 21%, the bead width by 11% and reinforcement by 39%.

A rise in travel speed reduces the heat input per unit length. It reduces the melting of the base metal thereby reducing the penetration [17, 22]. The reduced heat input also lowers the metal deposition rate per unit length. With the reduction in heat input and the metal deposition rate, the overall size of the weld pool goes down, which in turn reduces the values of bead width, penetration and reinforcement [18]. However, since there is no change in the arc voltage and hence the shape of the arc cone, the reduction in the bead width is solely due to the overall reduction in the weld pool size, therefore it is marginal (11%).

Figure 9(a) and (b) depict the interactive effects of welding current (I) and the travel speed (S) on the bead width (w) and reinforcement (r) of the welds. From these figures, it can be observed that these two parameters exerts almost similar interactive effects on these two elements. Further, the effect is more pronounced at lower values of S and higher values of I, due to the combined effect of these variables [26, 37].

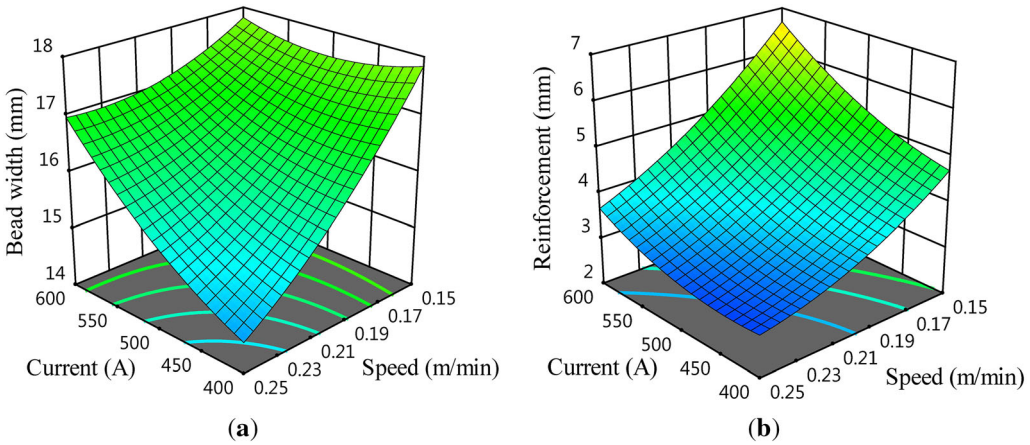

Figure 9. Interactive effects of current and travel speed on (**a**) bead width and (**b**) reinforcement.

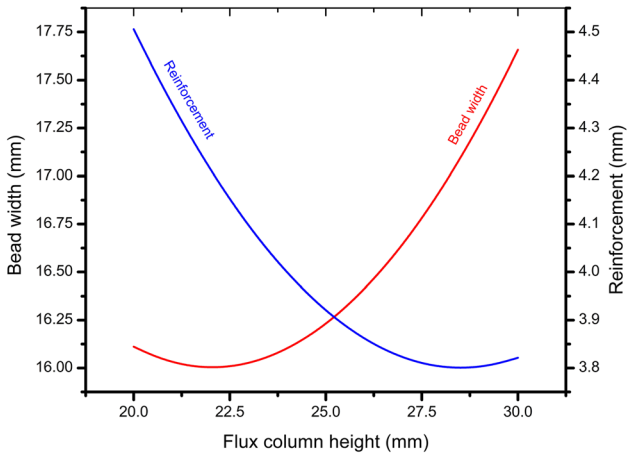

Figure 10. Influences of column height.

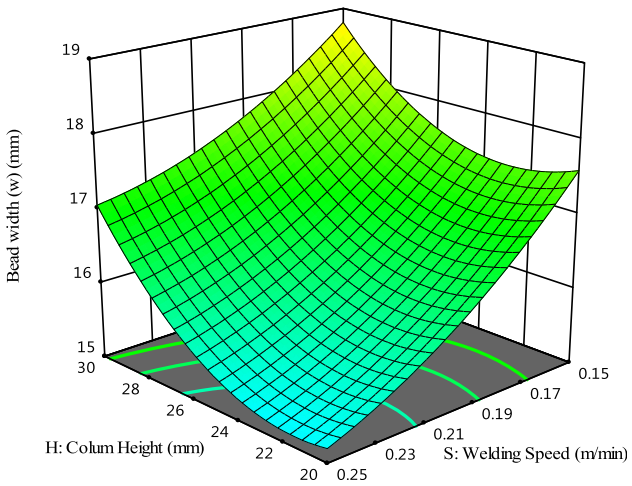

Figure 11. Interactive effects of travel speed and flux column height on the bead width.

3.4 *Effects of column height*

Flux column height is the height of the flux column above the welding arc cavity. Practically it is taken as the height of the flux column above the surface of the workpiece. The observed effects of column height on various bead geometry parameters have been quantified mathematically in Eqs. (1) to (3). These are depicted graphically in figure 10. During the experimentation, the flux height was increased by 50% i.e. from 20 mm to 30 mm. This variation increased the bead width by 10%, coupled with a 15% decrease in reinforcement.

The flux column height is an important factor that has a considerable influence on the permeability of the flux layer above the arc cavity. An increase in the column height reduced the permeability considerably. As a result, the gases in the arc cavity find it difficult to escape into the atmosphere. Consequently, these gases exert a larger pressure upon the top surface of the molten weld pool and the

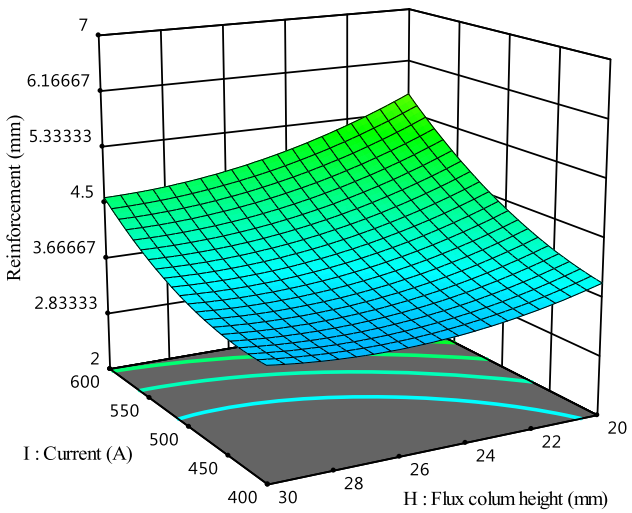

Figure 12. Interactive effects of welding current and flux column height on reinforcement.

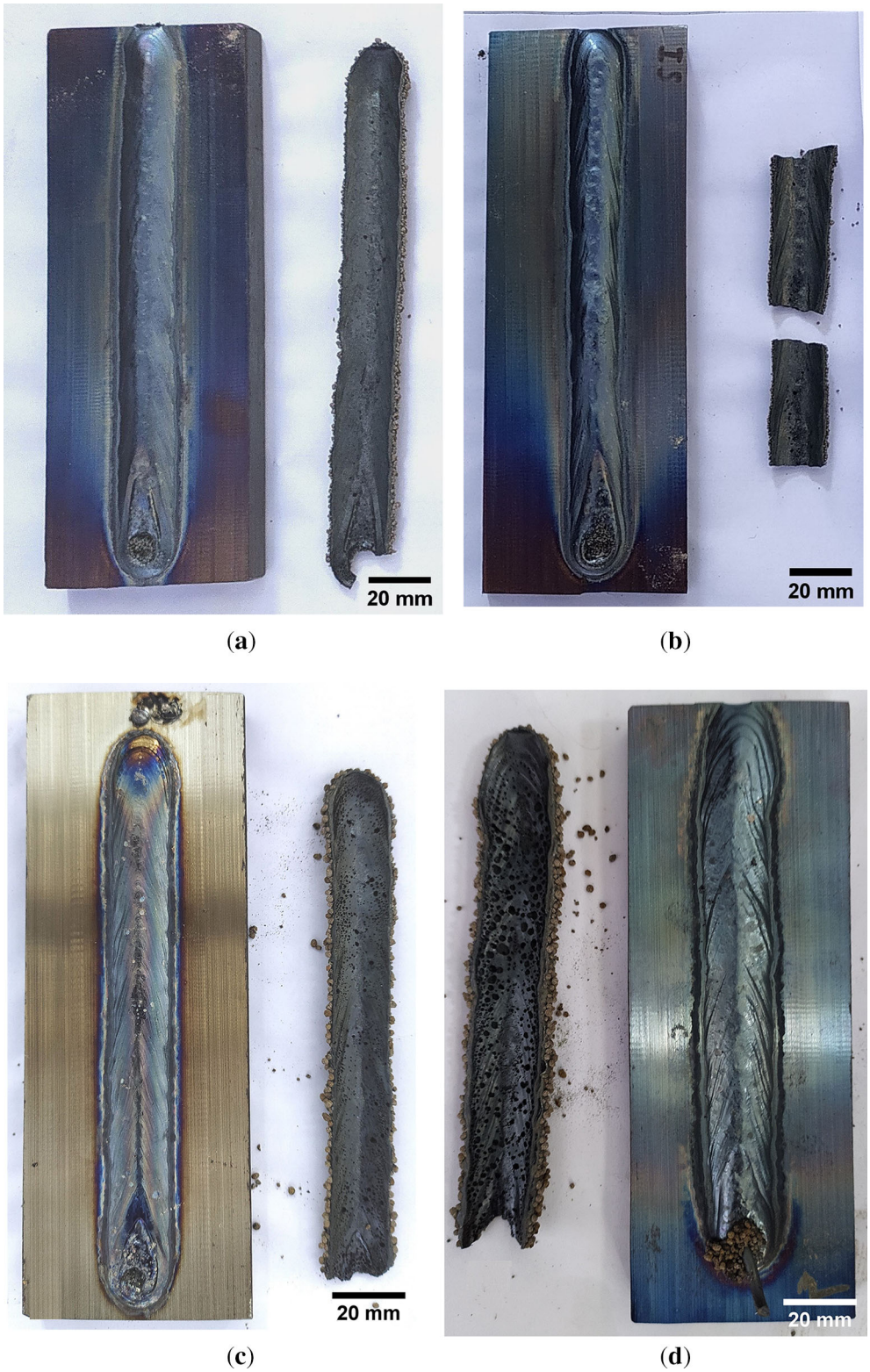

(**a**) (**b**)

(**c**) (**d**)

Figure 13. Weld beads deposited with (**a**) course flux at lower column height, (**b**) fine flux with lower column height, (**c**) course flux with higher column height and (**d**) fine flux with higher column height.

inner side of the molten slag [31, 32]. This additional gas pressure is primarily responsible for the reduction in reinforcement and a corresponding enhancement of the bead width [38]. These gases also induce several defects like blowholes, porosity, and poke marks in the weld bead, as depicted in figures 13 (c and d).

Besides the above factor, the increased height of the flux column also adds extra weight above the molten weld pool. This extra weight also contributes to a further reduction in the reinforcement and the increase in bead width [31].

Figure 11 depicts the interactive effect of flux column height (H) and the travel speed (S) on the bead width (w) of the welds. In general, S has a negative effect on w, while H has a positive effect on it. It can be observed that the rate of decrease in the value of w with the increase in S is reduced as the value of H is increased. It is probably because, with the increase in height of the flux layer (column) the weld pool becomes more insulated. It reduces the heat losses from the weld pool. Consequently, the rate of reduction in the bead width is decreased.

Figure 12 shows the interactive effects of welding current (I) and flux column height (H) on the reinforcement (r) of the welds. The graph depicts an increase in the value of column height (H) reduced reinforcement (r), at higher as well as lower values of current (I). However, at a higher value of current (I), the effect of flux column height (H) becomes less pronounced. It is probably due to the fact that at elevated temperatures, the fluidity of the molten flux layer increases due to an increase in the heat input [31, 32]. It makes the escapes of the arc gases comparatively easier, thereby relieving the excessive pressure above the weld pool. As a result, the effect of flux column height on the reinforcement is reduced.

3.5 *Effects on surface appearance*

The influences of flux particle size and column height on the surface appearance of the SAW welds could be understood by closely observing figures 13(a) to (d). These figures show the upper surfaces of various weld beads deposited at various combinations of the flux particle size and flux column height. These figures also show the surfaces of the slag strips removed from the beads, for a better understanding.

By the comparison of these figures, it can be observed that the weld beads deposited at a lower flux height possess a better surface finish, display finer ripples, and are free from all types of surface defects. A further comparison of figures 13(a) and (b) reveals that even for the welds deposited at low flux height, the surface finish of the beads deposited with the course flux is better than those deposited with finer flux.

On the other hand, the surface finish of the beads deposited with larger flux column height is inferior as depicted in figures 13 (c and d). The surface appearance of the beads deposited with larger flux column height and finer particle size (figure 13 (d)) is the worst, with large visual defects like pinholes and poke marks present on the surface.

At low flux column height, the gases produced in the arc cavity could easily escape into the atmosphere, as the flux layer is thin. Consequently, a smooth weld bead with fine ripples is deposited. It is also evident from the smooth inner surface of the slag strips removed from these welds [32, 39]. As the height of the flux column is increased, a thicker layer of flux particles is formed above the molten flux. It prevents the release of gases from the arc cavity. The gas pressure continues to grow until it reaches a critical value. At that point, the flux layer bursts momentarily and the arc gases are released [32, 38]. This phenomenon happens intermittently and causes the formation of irregular ripples on the surface of weld beads, as are visible in figure 13 (d).

If we carefully observe the inner surface of the slag strips removed from these beads, we may readily notice the presence of a large number of gas holes. These holes have been formed by arc gases that could not escape through the flux layer before the solidification of the slag [30, 38]. These gas bubbles produce many types of surface defects such as porosity, blow holes, pin holes, and poke marks [38], some of which are also visible in figure 13 (d).

4. Conclusions

A systematic investigation was undertaken to study the effects of flux particle size and column height on the bead geometry in the submerged arc welding process. The following conclusions could be drawn:-

I. In the submerged arc welding process, the particle size of the flux and the flux column height above the arc cavity, exert significant influence on the bead profile of the welds.
II. A 100% increase in average flux particle size reduced the bead width by 9% and enhanced the reinforcement by 12%. On the contrary, a 50% elevation in the flux height increased the bead width by 10% and decreased the reinforcement by 15%. However, none of these two parameters could exert any significant effects on penetration.
III. The welding current exerted a positive effect on all the elements of the bead geometry. A 50% increase in welding current could increase the penetration by 60%, bead width by 15% and reinforcement by 40%.
IV. Contrary to the above, the travel speed registered a negative effect on all these elements. A 66% escalation in travel speed reduced the penetration by 21%, bead width by 11% and reinforcement by 39%.
V. The flux particle size and column height also exert a significant influence on the surface quality of the SAW

welds. The welds produced with a low flux column height exhibit a good surface finish irrespective of the particle size of the flux. While the surface appearance of the welds made with a larger flux column is greatly dependent upon the flux particle size.

References

[1] Patel D and Soman S 2020 Develop a flux cored wire for submerged arc welding of Ni-Mo low alloy steel. *Sadhana.* 45(1): 1–10

[2] Saini S and Singh K 2021 Recycling of steel slag as a flux for submerged arc welding and its effects on chemistry and performance of welds. *Int. J. Adv. Manuf. Technol.* 114(3): 1165–1177

[3] Coetsee T and De Bruin F J 2022 Improved Titanium Transfer in Submerged Arc Welding of Carbon Steel through Aluminum Addition. *Miner. Process. Extr. Metall. Rev.* 43(6): 771–774

[4] Choudhary A, Kumar M, Gupta M K, Unune D K and Mia M 2020 Mathematical modeling and intelligent optimization of submerged arc welding process parameters using hybrid PSO-GA evolutionary algorithms. *Neural. Comput. Appl.* 32(10): 5761–5774

[5] Garg J and Singh K 2016 Slag recycling in submerged arc welding and its effects on the quality of stainless steel claddings. *Mater. Des.* 108: 689–698

[6] Gunaraj V and Murugan N 1999 Prediction and comparison of the area of the heat-affected zone for the bead-on-plate and bead-on-joint in submerged arc welding of pipes. *J. Mater. Process. Technol.* 95(1–3): 246–261

[7] Chandel R, Seow H and Cheong F 1997 Effect of increasing deposition rate on the bead geometry of submerged arc welds. *J. Mater. Process. Technol.* 72(1): 124–128

[8] Han X, Li C, Chen X and Jia S 2022 Numerical simulation and experimental study on the composite process of submerged arc cladding and laser cladding. *Surf. Coat. Technol.* 439: 128432

[9] Singh B, Khan Z A, Siddiquee A N and Maheshwari S 2018 Experimental study on effect of flux composition on element transfer during submerged arc welding. *Sadhana.* 43(2): 26

[10] Moinuddin S Q and Sharma A 2019 Multiple-Wire Welding GMAW and SAW. in *Advances in Welding Technologies for Process Development.* ed: CRC Press, pp. 1–22

[11] Srikarun B, Oo H Z, Petchsang S and Muangjunburee P 2019 The effects of dilution and choice of added powder on hardfacing deposited by submerged arc welding. *Wear.* 424: 246–254

[12] Sarfudeen M and Muthukumaran S 2020 Effect of cold wire addition on improvement in productivity by submerged arc welding in wind turbine tower fabrication. *Mater Today.* 27: 2699–2702

[13] Ferreira dos Santos N, Esteves L, Nery Garcia J H, Junior R C, Modenesi P J and Pereira da Silva B *et al.* 2020 Microstructural and corrosion resistance of lean duplex stainless steel UNS S32304 welded by SAW with cold wire addition. *Corros.* 76(7): 619–627

[14] Cevik B, Sahin O and Gulenc B 2021 Flux cored arc welding on 30MnB5 steels used in agricultural mechanisation: microstructure evolutions and mechanical properties. *Sadhana.* 46(3): 1–10

[15] Om H and Pandey S 2013 Effect of heat input on dilution and heat affected zone in submerged arc welding process. *Sadhana.* 38(6): 1369–1391

[16] Sarkar A, Dey P, Rai R and Saha S C 2016 A comparative study of multiple regression analysis and back propagation neural network approaches on plain carbon steel in submerged-arc welding. *Sadhana.* 41(5): 549–559

[17] Kumar A and Singh K 2020 Development of Exothermic Flux for Enhanced Penetration in Submerged Arc Welding. *J. Adv. Manuf. Syst.* 19(01): 131–146

[18] Murugan N and Gunaraj V 2005 Prediction and control of weld bead geometry and shape relationships in submerged arc welding of pipes. *J. Mater. Process. Technol.* 168(3): 478–487

[19] Yang L, Chandel R and Bibby M 1993 The effects of process variables on the weld deposit area of submerged arc welds. *Weld. J.* 72: 11-s

[20] Garg J and Singh K 2016 Effects of Process Parameters and Recycled Slag on Flux Consumption in Submerged Arc Stainless Steel Cladding. *Indian. J. Sci. Technol.* 9: 28

[21] Singh J, Singh K and Garg J 2011 Reuse of slag as flux in submerged arc welding & its effect on chemical composition, bead geometry & microstructure of the weld metal. *Int. J. Surf. Eng. Mater Technol.* 1(1): 4

[22] Yang L, Chandel R and Bibby M 1993 The effects of process variables on the weld deposit area of submerged arc welds. *Weld. J.* 72: 11s–18s

[23] Tarng Y and Yang W 1998 Application of the Taguchi method to the optimization of the submerged arc welding process. *Mater. Manuf. Process.* 13(3): 455–467

[24] Gunaraj V and Murugan N 1999 Application of response surface methodology for predicting weld bead quality in submerged arc welding of pipes. *J. Mater. Process. Technol.* 88(1–3): 266–275

[25] Gunaraj V and Murugan N 2000 Prediction and optimization of weld bead volume for the submerged arc process—part 1. *Weld. J.* 79(10): 286s–294s

[26] Kanjilal P, Pal T and Majumdar S 2006 Combined effect of flux and welding parameters on chemical composition and mechanical properties of submerged arc weld metal. *J. Mater. Process. Technol.* 171(2): 223–231

[27] Karaoglu S and Secgin A 2008 Sensitivity analysis of submerged arc welding process parameters. *J. Mater. Process. Technol.* 202(1–3): 500–507

[28] Choudhary A, Kumar M and Unune D R 2019 Experimental investigation and optimization of weld bead characteristics during submerged arc welding of AISI 1023 steel. *Def. Technol.* 15(1): 72–82

[29] Siewert T and Franke G 1990 Analysis and Characterization of Commercial Welding Fluxes. *Weld. J.* 69(7): 247

[30] Mathers G 2020 *Job Knowledge 87*. Available: https://www.twi-global.com/technical-knowledge/job-knowledge/submerged-arc-welding-consumables-part-1-087

[31] Patel N 2020 *Submerged Arc Welding Fluxes: The criticality of particle size*. Available: https://www.welding-advisers.

com/submerged-arc-welding-fluxes-the-criticality-of-particle-size1.html

[32] Kumagai M and Okuda N 1986 Research on Bead Formation in Submerged Arc Welding. III. Effect of Flux Height on the Bead Appearance in Submerged Arc Welding. *Q. J. Jpn. Weld. Soc.* 4(2): 283–289

[33] Senthilkumar B, Kannan T and Madesh R 2017 Optimization of flux-cored arc welding process parameters by using genetic algorithm. *Int. J. Adv. Manuf. Technol.* 93: 35–41

[34] Mishra D, Manjunath A and Parthiban K 2021 Experimental investigation and optimization on interpulse welding of Nimonic C263 for the maximum tensile strength. *Sadhana.* 46(3): 1–12

[35] Sharma S K, Maheshwari S and Singh R K R 2019 Effect of heat-input and cooling-time on bead characteristics in SAW. *Mater. Manuf. Process.* 34(2): 208–215

[36] Saha M K, Hazra R, Mondal A and Das S 2019 Effect of heat input on geometry of austenitic stainless steel weld bead on low carbon steel. *J. Inst. Eng. (India): C.* 100(4): 607–615

[37] Tusek J, Umek I and Bajcer B 2005 Weld-cost saving accomplished by replacing single-wire submerged arc welding with triple-wire welding. *Sci. Technol. Weld. Join.* 10(1): 15–22

[38] Rao R V and Rai D P 2017 Optimization of submerged arc welding process parameters using quasi-oppositional based Jaya algorithm. *J. Mech. Sci. Technol.* 31(5): 2513–2522

[39] Sharma L, Kumar J and Chhibber R 2020 Experimental investigation on surface behaviour of submerged arc welding fluxes using basic flux system. *Ceram. Int.* 46(6): 8111–8121